Acta Cryst. (1998). A**54**, 886–894

Determination of X-ray Reflection Phases Using *N*-Beam Diffraction

Shih-Lin Chang

Department of Physics, National Tsing Hua University and Synchrotron Radiation Research Center, Hsinchu, Taiwan. E-mail: slchang@phys.nthu.edu.tw

(*Received 20 January 1998; accepted 22 June 1998*)

Abstract

The relationship between X-ray reflection phase and *N*-beam diffraction as well as the phase-determination method utilizing *N*-beam interference effects are described. The experimental techniques of producing *N*-beam diffraction and the theoretical grounds, both kinematical and dynamical, of the phase-determination method are presented and discussed. Experimental phase determination using *N*-beam diffraction for single crystals of small molecules and macromolecules is demonstrated. Prospective future development of this particular phasing method is also given.

1. Introduction

Phase, a relative physical quantity, usually plays a very important role in many systems. For X-ray diffraction from crystals, the phases as well as the amplitudes of X-ray reflections are decisive information needed for the determination of crystal structures. Unfortunately, this phase information is lost in X-ray diffraction measurements because the detected intensity of a single Bragg reflection is only proportional to the product of the involved structure factor and its complex conjugate, where the structure factor is the diffracted amplitude and phase of a crystal unit cell. This fact constitutes the well known X-ray phase problem in crystallography, diffraction physics and X-ray optics. Solutions to this problem have been developed considering the physical and statistical aspects of two-beam Bragg reflections. These include direct methods (see, for example, Schenk, 1991, and references therein), methods involving isomorphous and molecular replacements (Rossmann, 1972), anomalous dispersion (Hendrickson, 1991), entropy maximization (Bricogne & Gilmore, 1990) and many others (Woolfson & Fan, 1995, and references therein).

Phases are usually measured by interference techniques. X-ray diffraction from crystals has been considered as an interference phenomenon of electromagnetic waves with three-dimensional gratings. It is, therefore, natural to think of using X-ray interference to determine the relative phases of X-ray reflections, where at least two diffracted waves with comparable amplitudes are required. Historically, this kind of thinking has indeed been implemented in real experiments attempting to solve the phase problem. In 1949, Lipscomb, among others, investigated the possibility of using *N*-beam diffraction for phase determination. The idea is the following: Consider a three-beam ($N = 3$) diffraction, in which one incident beam and two diffracted beams are involved. One of the diffracted beams can be treated as a reference for the other diffracted beam as long as the two diffracted beams appear simultaneously. The interference between the two modifies the intensities of the diffracted beams. The intensity variation in each of the diffracted beams carries the phase information, which can be extracted from the intensity analysis. This idea has been further adopted in electron and X-ray diffraction experiments (for reviews, see Chang, 1987, and references therein; Colella, 1992; Weckert & Hümmer, 1997, and references therein). Applications of this phase-determination method to organic and macromolecular crystals have recently been realised as well. In what follows, the geometry, the experimental techniques and the theoretical grounds of *N*-beam diffraction are briefly described. For illustration, phase determinations from the intensity measurements of *N*-beam interference in small and macromolecular crystals are presented. The accuracy and applicability of this phasing method for structure analysis are discussed. Possible future development is also tentatively given.

2. *N*-beam X-ray diffraction

N-beam multiple diffraction takes place when $N - 1$ sets of atomic planes are simultaneously brought into posi-

S.-L. Chang has a PhD in Physics (1975) from the Polytechnic Institute of Brooklyn, New York. He is currently Professor of Physics, National Tsing Hua University, Hsinchu, Taiwan. He taught physics at Universidade Estadual de Campinas in Brazil (1975–1985) as Assistant Professor, Associated Professor and Professor. He was a visiting scientist at the Max-Planck Institut für Festkorperforschung (1981–1982) and Brookhaven National Laboratory (1991). His main research interests are X-ray dynamical diffraction, multiple diffraction, the phase problem and synchrotron-related topics.

tion to diffract an incident beam. The total number of beams, N, consists of the incident beam and the $N-1$ diffracted beams. In terms of the reciprocal lattice, N reciprocal-lattice points (r.l.p.'s), O, G_1, G_2, ..., G_{N-1}, are on the surface of the reflection sphere, the Ewald sphere, with radius $1/\lambda$, λ being the X-ray wavelength used (Cole *et al.*, 1962). The vector from the center of the sphere to each r.l.p. is the wave vector indicating the direction of a diffracted beam. For example, Figs. 1(*a*) and (*b*) show the geometry of a three-beam (O, G, L) diffraction in real space and reciprocal space, respectively. $\mathbf{K}_O$, $\mathbf{K}_G$ and $\mathbf{K}_L$ are the wave vectors of the incident and the diffracted beams. Since the modulus of the reciprocal-lattice vector (r.l.v.) $\overrightarrow{OG}$ equals $1/d_G$, d_G being the interatomic distance of the G planes, Bragg's law is likewise satisfied, *i.e.* $2d_G \sin\theta_G = \lambda$, where θ_G is the Bragg angle of the G reflection. The same is true for all the r.l.p.'s on the surface of the Ewald sphere as shown in Fig. 1(*b*).

Three-beam diffraction can be systematically generated by first aligning the crystal for the G reflection, the primary reflection, to bring the r.l.p. G onto the surface of the Ewald sphere (Figs. 1*a* and *b*), and then rotating the crystal around the r.l.v. $\overrightarrow{OG}(=\mathbf{g})$ to bring additional r.l.p.'s (of secondary reflections) to touch the surface of the Ewald sphere. During the ψ rotation, there are two positions for a given three-beam diffraction to occur, *i.e.* the IN and OUT positions, at which the r.l.p. of the secondary reflection enters and leaves the Ewald sphere, respectively. The phase change in the three-beam diffraction process is closely related to the three-beam interaction inside the crystal. As shown in Fig. 1(*c*), the incident beam is reflected simultaneously by the G and L planes. The L-reflected beam is rescattered back to the G reflected direction *via* the coupling of the $G-L$ reflection and interferes with the G-reflected beam. This coherent three-beam interaction thus modifies the intensity of each diffracted beam, which then depends, without considering anomalous dispersion, on the phase sum of the $-G$, L and $G-L$ reflections, *i.e.* the phase δ_3 of the structure-factor triplet $F_{-G}F_LF_{G-L}$. By definition, the structure factor F_{-G} of the G reflection is given as

$$F_G = \sum_j f_j \exp[2\pi i(\mathbf{g}\cdot\mathbf{r}_j)], \tag{1}$$

where f_j and $\mathbf{r}_j$ are the atomic scattering factor and the relative position vector of the jth atom in the crystal unit cell, respectively. Since the r.l.v.'s $-\overrightarrow{OG}$, $\overrightarrow{OL}$ and $\overrightarrow{LG}$ in Fig. 1(*b*) form the OLG triangle, namely $-\mathbf{g}+\mathbf{l}+(\mathbf{g}-\mathbf{l})=0$, the phase δ_3 is independent of the choice of the origin of the unit cell. It is this invariant phase that is physically meaningful.

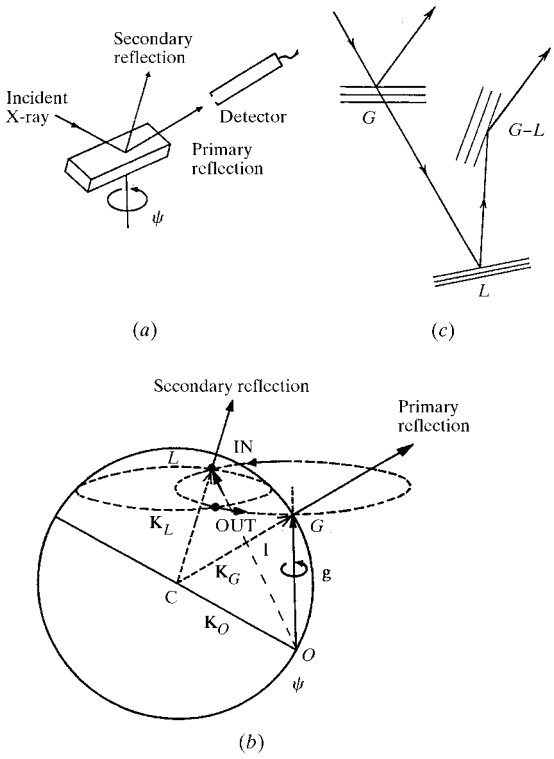

Fig. 1. Three-beam diffraction geometry in (*a*) real space and (*b*) reciprocal space; (*c*) schematic of three-beam interaction. (The interaction takes place simultaneously everywhere all over the crystal.)

Two main techniques can be used to generate an N-beam diffraction: the Renninger technique using a collimated incident beam of a few arc minutes of divergence (Renninger, 1937) and the Kossel technique with a divergent beam of 5 to a few tens of degrees (Kossel, 1936). The former usually adopts a scintillation counter to monitor the multiply diffracted beams during the ψ rotation of the crystal around the $\mathbf{g}$ vector (Fig. 1*a*), whereas the latter employs X-ray films or area detectors to record the two-dimensional intensity distribution while the crystal remains stationary (Fig. 3*a*). Figs. 2 and 3(*b*) are the multiple diffraction pattern of silicon (222) of Cu $K\alpha_1$ obtained with the Renninger technique and the image of germanium four-beam (000, 004, $\bar{1}\bar{1}1$, $\bar{1}\bar{1}3$) diffraction of Cu $K\alpha$ radiation with the Kossel technique, respectively. In Fig. 2, the background is the diffracted intensity of the primary 222 reflection, and the peaks indicate the multiple diffractions, of which the Miller indices of the involved secondary reflections are given. In Fig. 3(*b*), the two horizontal lines are the images of the 004 reflection for Cu $K\alpha_1$ and Cu $K\alpha_2$ and the two arrows labeled ($\bar{1}\bar{1}1$) and ($\bar{1}\bar{1}3$) represent the directions of the $\bar{1}\bar{1}1$ and $\bar{1}\bar{1}3$ reflections. The intersections of the ($\bar{1}\bar{1}1$) and ($\bar{1}\bar{1}3$) lines with the (004) images are the locations at which the four-beam (000, 004, $\bar{1}\bar{1}1$, $\bar{1}\bar{1}3$) diffractions of Cu $K\alpha_1$ and Cu $K\alpha_2$ take place. Intensity modification in the vicinity of the four-beam points is clearly observed. Compared with the divergent-beam technique, Fig. 3(*c*) shows the

corresponding multibeam diffraction pattern obtained with the Renninger geometry.

3. Theoretical foundation

The intensity distribution of an *N*-beam diffraction can be accounted for using the dynamical theory and kinematical theory of X-ray diffraction, depending on whether the crystal is perfect or imperfect. Since the intensity variation in an *N*-beam diffraction is due mainly to the coherent dynamical interaction among the diffracted beams, we shall first briefly outline the dynamical theory for *N*-beam cases. For details, the readers should refer to the books and review articles by Authier *et al.* (1996), Batterman & Cole (1964), Ewald & Heno (1968), Kato (1974, and references therein), Colella (1974), Pinsker (1978), Chang (1984), and many others.

X-ray diffraction from a crystal can be described by Maxwell's equations, where the crystal is treated as a complex periodic medium and the wave vectors satisfy Bragg's law, *i.e.* $\mathbf{K}_G = \mathbf{K}_O + \mathbf{g}$ for $G = G_1, G_2, \ldots, G_{N-1}$ and $g = g_1, g_2, \ldots, g_{N-1}$. The solution of the equations leads to the so-called fundamental equations of wave fields in the plane-wave approximation:

$$(k^2 - K_G^2)\mathbf{D}_G = \sum_H \chi_{G-H}[\mathbf{K}_G \times (\mathbf{K}_G \times \mathbf{D}_H)], \quad (2)$$

where $\mathbf{D}_G$ and $\mathbf{K}_G$ are the electric displacement and the wave vector of the G reflection inside the crystal, respectively, and $k = 1/\lambda$. There are $4N$ equations of (2), if both the σ and π polarizations of the wave fields are considered. For the nontrivial solutions of the D's of the $4N$ linear equations of (2), the determinant of the coefficients of the D's must be null. This establishes the dispersion relation between the wave vectors **K** and the angles $\Delta\theta$ and $\Delta\psi$, where $\Delta\theta$ and $\Delta\psi$ are the angular deviations from the Bragg angle θ_G and the exact *N*-beam azimuthal angle ψ_o, respectively.

Equation (2) can be solved as an eigenvalue problem. The real parts of the eigenvalues define the dispersion surface in reciprocal space, and the imaginary parts yield the linear absorption coefficients. The eigenvectors are the ratios of the wave-field amplitudes among the diffracted beams. Both the eigenvalue and the corresponding eigenvector specify a normal mode of X-ray wave propagation. The diffracted intensity can be calculated, as usual, from appropriate boundary conditions, *i.e.* the continuities of the normal components of **D** and **B** and of the tangential components of **E** and **H** at the crystal boundaries.

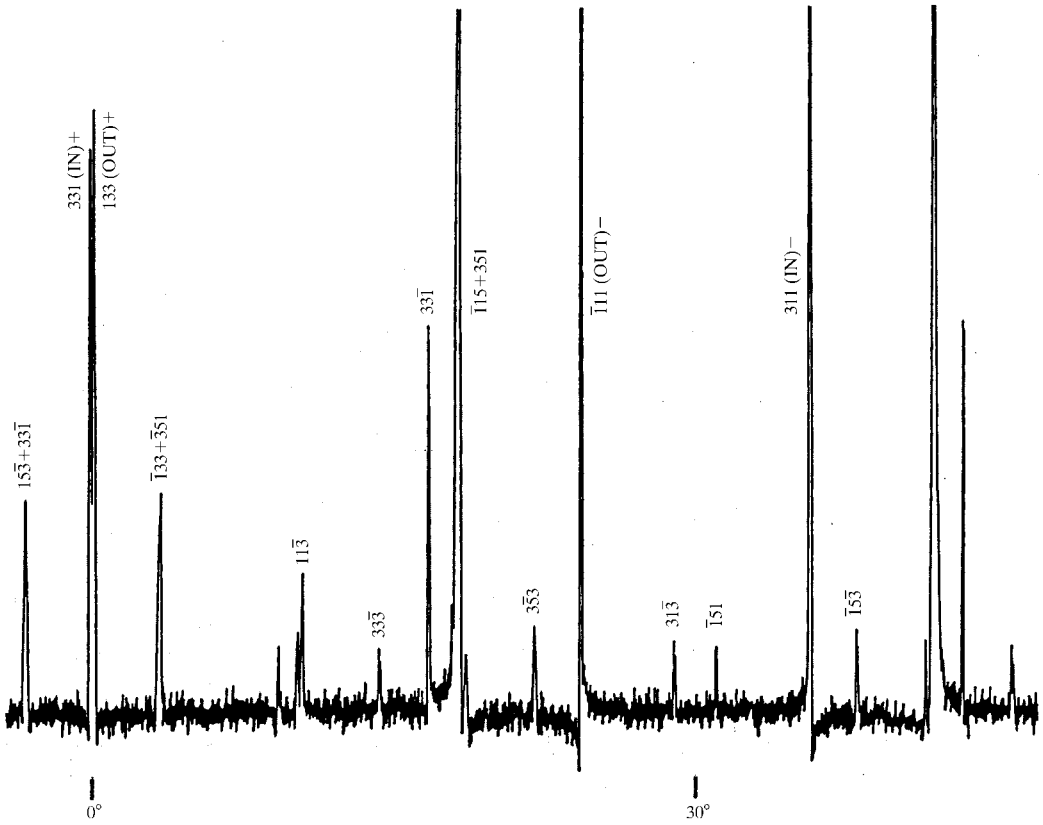

Fig. 2. *N*-beam diffraction pattern of silicon (222) with Cu $K\alpha_1$ radiation.

The phases and magnitudes of the structure factors involved and the angular position of the incident beam, defined by $\Delta\theta$ and $\Delta\psi$, are the input data for the dynamical calculations of the diffracted intensities. However, to solve the phase problem, we need to determine phases from measured intensities. Hence, an analytical expression relating intensity to phase is desired. Unfortunately, such an expression does not exist for a general N-beam diffraction, unless some approximation is employed. Under the second-order Born approximation (or Bethe approximation), the wave field $\mathbf{D}_G(3)$ of a three-beam (O, G, L) diffraction can be expressed in terms of the two-beam wave field (Juretschke, 1982*a*,*b*; Hoier & Marthinsen, 1983; Chang, 1984; Hümmer & Billy, 1982, 1986; Shen, 1986; Thorkildsen, 1987; Mo *et al.*, 1988):

$$\mathbf{D}_G(3) = \mathbf{D}_G(2)[1 + R_L\Gamma|F_{G-L}F_L|/|F_G|\exp(i\delta_3)] \quad (3)$$

with $R_L = k^2/(k^2 - K_L^2)$, where $\Gamma = -r_e\lambda^2(\pi V)^{1/2}$, r_e is the classic radius of the electron and V the volume of the crystal unit cell. R_L is the excitation function. According to Ewald (1965), X-ray diffraction is a spatial resonance phenomenon, analogous to temporal resonance involving frequencies. Thus, R_L can be represented by the familiar resonance function given below (Hümmer & Billy, 1986):

$$R_L = 1/[\Delta\psi + i(\eta_i/2)], \quad (4)$$

where η_i is the fundamental width of the three-beam diffraction, which is related to scattering and absorption. The corresponding relative intensity distribution convoluted with the crystal mosaic spread η_m and the instrumental broadening η_b takes the form (Chang & Tang, 1988)

$$I_G = [I_G(3) - I_G(2)]/I_G(2) = I_D + I_K, \quad (5)$$

where

$$I_D = A[2(\Delta\psi)\cos\delta_3 - \eta\sin\delta_3]/[(\Delta\psi)^2 + (\eta/2)^2]^{1/2} \quad (6)$$

$$I_K = C\{(\eta/2)^2/[(\Delta\psi)^2 + (\eta/2)^2]\}. \quad (7)$$

$I_G(2)$ and $I_G(3)$ are the two-beam and the three-beam intensities of the primary G reflection, respectively. The quantities A and C depend on the structure-factor moduli, Lorentz–polarization factor and $\Delta\psi$. I_K is a symmetric function of $\Delta\psi$. The total peak width is $\eta = \eta_i + \eta_b + \eta_m$ for a Lorentzian profile.

In deriving (5), the intensity $I_G(3)$ takes the product of $\mathbf{D}_G(3)$ and its complex conjugate, which is related to the sum of the structure-factor triplet $F_{-G}F_LF_{G-L}$ and its complex conjugate. Assuming negligibly small anomalous-dispersion effects, these two structure factors are identical. Thus, the dynamical intensity I_D in (6) depends on the phase δ_3 of the $F_{-G}F_LF_{G-L}$, whereas the kinematical intensity I_K is phase independent. Moreover, I_D is related to the real part, $\mathrm{Re}[R_L]$, and the imaginary part, $\mathrm{Im}[R_L]$, of the excitation function R_L as

$$I_D = A\{\cos\delta_3\,\mathrm{Re}[1/(\Delta\psi + i\eta)] + \sin\delta_3\,\mathrm{Im}[1/(\Delta\psi + i\eta)]\}. \quad (8)$$

That is, I_D is, in reality, a function of the effective phase u defined as $u = \delta_3 + \arctan(\eta/2/\Delta\psi)$. Furthermore, the real part and imaginary part of I_D satisfy the Kramers–Kronig relation (Tang & Chang, 1990). Fig. 4 shows the calculated intensity I_G', the kinematical I_K, the dynamical I_D, the Kramers–Kronig transformed I_D, denoted as $K[I_D]$, and the effective phase u for various triplet phase values. The asymmetry of the I_D profile *versus* $\Delta\psi = 0$ clearly reflects the phase effects on the diffracted intensity profiles. Also, the value of u for large $\Delta\psi$ is the corresponding triplet phase value δ_3. Moreover, the relation $K[I_D(\delta_3)] = I_D(\delta_3 - 90^\circ)$ is also revealed, indicating the connection between the real part and the imaginary part of the phase-dependent profiles I_D.

Strictly speaking, this derivation by using the Born approximation is a kinematical approach. In addition,

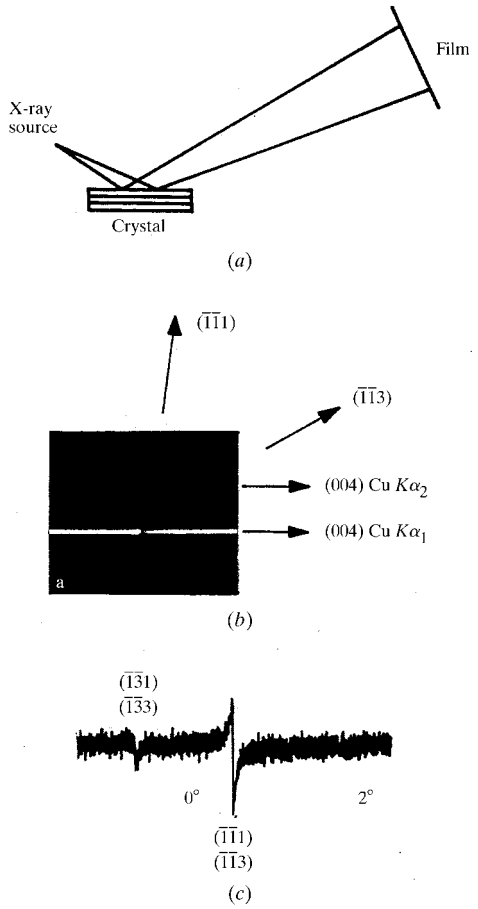

Fig. 3. Divergent-beam (Kossel) technique: (*a*) the experimental set-up and (*b*) intensity distribution of Ge (004) in the four-beam (000, 004, $\bar{1}\bar{1}1$, $\bar{1}1\bar{3}$) case. (*c*) Intensity distribution of (*b*) along the (004) Cu $K\alpha_1$ line obtained with a collimated incident beam.

the I_K should, in principle, be governed by the power-transfer equations of the kinematical theory (Moon & Shull, 1964; Zachariasen, 1965; Caticha-Ellis, 1969):

$$\pm \mathrm{d}P_i/\mathrm{d}x = -\mu P_i/\gamma_i + \sum_j (Q_{ji}P_j/\gamma_j - Q_{ij}P_i/\gamma_i), \quad i \neq j,$$

where P_i, μ and γ_i are the diffracted power, the linear absorption coefficient and the direction cosine with respect to the crystal normal of the reflection i, respectively. The term Q_{ij}, proportional to $|F_{ij}|^2$, is the reflectivity of the reflection $i - j$. The subscripts i and j can be any one of the O, G and L reflections.

4. Phase determination from *N*-beam intensity measurements

Single crystals with and without a center of inversion are called centrosymmetric and noncentrosymmetric crystals, respectively (Hargittai, 1998). Reflections with phases equal to 0 or 180° are centric reflections, while those with phases between 0 and 360° are acentric reflections. For a three-beam diffraction, which involves centric and acentric reflections, the triplet phase can, in principle, be determined by comparing the experimentally obtained profiles with the calculated ones shown in Fig. 4. In practice, the phases of centric reflections can be determined qualitatively according to the sign of $\cos\delta_3$ (Post, 1977). For acentric reflections, quantitative analysis of phases is needed. These two phase-determination procedures are described below.

4.1. *Qualitative phase determination*

Referring to Figs. 4(*a*) and (*b*), if the intensity I'_G decreases at lower angles and increases at higher angles, then the phase δ_3 is equal or close to 0°. The reverse is true for $\delta_3 = 180°$ (Chapman *et al.*, 1981). Moreover, the profile asymmetry is reversed as $\Delta\psi$ changes sign.

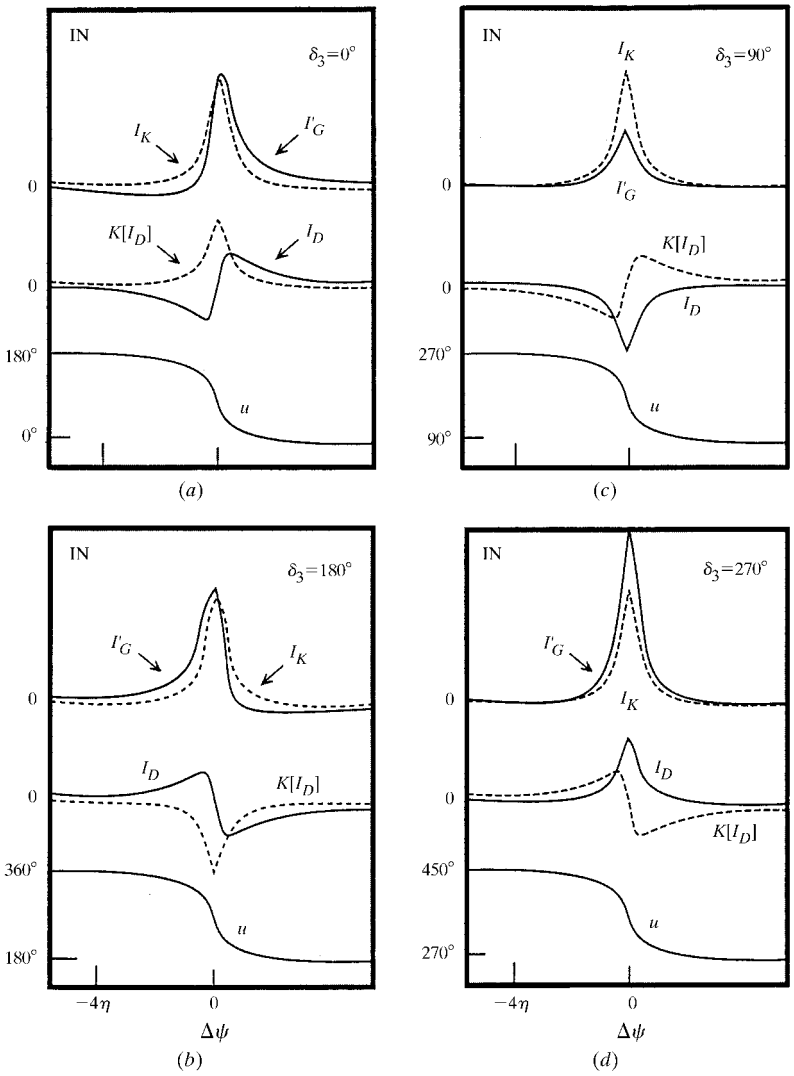

Fig. 4. Calculated I'_G, I_K, I_D, $K[I_D]$ and u *vs* $\Delta\psi$ of a three-beam case for various δ_3 values at the IN situations.

Varying the value of $\Delta\psi$ from negative to positive and *vice versa* corresponds to the IN and OUT situations, where the same N-beam case takes place. This argument leads to the sign relation (Chang, 1982)

$$S(\cos\delta_3) = S_L S_R, \tag{9}$$

where S_L is positive for the intensity asymmetry of I'_G (or I_D) shown in Fig. 4(a) and negative for I'_G (or I_D) in Fig. 4(b). S_R is positive for the IN and negative for the OUT situation. In practice, the sign S_{GL} of $\mathbf{g}\cdot\mathbf{l} - l^2$ and the sign S_P of the polarization factor also affect the signs S_R and S_L, respectively (Shen, 1986). Thus, the useful sign relation becomes

$$S(\cos\delta_3) = S_L S_R S_{GL} S_P, \tag{10}$$

where S_P is determined by following the discussions given by Juretschke (1986), Shen & Finkelstein (1990), and Weckert & Hümmer (1997, and references therein).

As an example, the intensity profiles of the three-beam diffractions of silicon, $(000, 222, \bar{1}\bar{1}1)$ and $(000, 222, 311)$, indexed by the secondary reflections $\bar{1}11$ and 311, show clear asymmetry near $\psi = 30^\circ$ in Fig. 2. The sign of the profile is $S_L > 0$ for the $\bar{1}11$ peak because the intensity first decreases and then increases as ψ increases (see also Fig. 4a). The sign $S_L < 0$ for the 311 peak, because its intensity distribution shows opposite asymmetry to that of the $\bar{1}11$ peak. Since the $\bar{1}11$ peak occurs at its OUT position and the 311 peak at its IN position, the sign S_R is '$-$' for the $\bar{1}11$ and '$+$' for the 311 peak. The coupling between the 222 and $\bar{1}11$ reflections of the former three-beam case is the $222 - \bar{1}11 = 311$ reflection. Similarly, the coupling reflection is $\bar{1}11$ for the latter three-beam case. According to (9), the phase signs determined for the triplets $F(\bar{2}\bar{2}\bar{2})F(\bar{1}11)F(311)$ and $F(\bar{2}\bar{2}\bar{2})F(311)F(\bar{1}11)$ are both negative because $S = S_L(+)S_R(-) = -$ for the former case and $S = S_L(-)S_R(+) = -$ for the latter case.

As shown in Figs. 4(c) and (d), the peak intensity at $\Delta\psi = 0$ in the case with $\delta_3 = 90^\circ$ is weaker than that in the case with $\delta_3 = 270^\circ$ because the integrated intensity depends on I_D as shown in (5) and (6) and the I_D is negative for the former and positive for the latter. This indicates that the peak intensity is closely related to $\sin\delta_3$, which leads to a semiquantitative phase-determination procedure (Hümmer & Weckert, 1990; Weckert & Hümmer, 1990). Accuracy of $\pm 45^\circ$ in phase values can be achieved by directly comparing the measured profiles of two centrosymmetrically related three-beam diffractions with the theoretically calculated ones. Phase determination of macromolecular crystals using this semiquantitative procedure has been demonstrated (Hümmer *et al.*, 1991).

4.2. *Quantitative phase determination*

According to (5) and (6), the phase-dependent I_D can be obtained as $I_D(\Delta\psi) = I'_G(\Delta\psi) - I_K(\Delta\psi)$, if the $I_K(\Delta\psi)$ can be constructed from the experimental data. As shown in (7), I_K is a Lorentzian with a full width at half-maxima (FWHM) η and maximum amplitude C. The amplitude C can be determined by using either three-beam reflections of the same $\{hkl\}$ family (Tang & Chang, 1988) or two centrosymmetrically related three-beam diffractions (Chang *et al.*, 1991). Since the two approaches bear the same origin, only the latter is described below: Suppose that the two centrosymmetrically related three-beam cases are case (a) (O, G, L) and case (b) $(O, -G, -L)$, for which $\delta_3(a) = -\delta_3(b)$. According to (6) and (7), at the peak positions ($\Delta\psi = 0$) and with no anomalous dispersion, $I_D(a) = -I_D(b)$ and $I_K(a) + I_K(b) = [I'_G(a) + I'_G(b)]/2 = C$. Thus, the intensity distribution $I_K(\Delta\psi)$ can be constructed experimentally with the determined C and η. Once $I_K(\Delta\psi)$ is known, the quantitative phase determination is straightforward *via*

$$\tan\delta_3 = [-I_+ - I_-]/[I_+ - I_-], \tag{11}$$

where

$$\begin{aligned} I_\pm &= I_D(\Delta\psi = \pm\eta/2) \\ &= I'_G(\Delta\psi = \pm\eta/2) - I_K(\Delta\psi = \pm\eta/2) \end{aligned} \tag{12}$$

and $I_K(\Delta\psi = \pm\eta/2) = C/2$. The quadrant to which δ_3 belongs is determined by the signs of the numerator and the denominator of (11). The $I_\pm$ defined in (12) is valid only for the IN situations and $I_\pm$ must be replaced by $I_\mp$ for the OUT situations.

For illustration, the phase-analysis procedure based on (11) has been applied to organic crystals of $C_{25}H_{25}NO$ (space group $P2_12_12$, $a = 20.2992$, $b = 14.8558$, $c = 6.9830$ Å, orthorhombic) and macromolecular crystals of hen egg-white lysozyme ($P4_32_12$, $a = b = 78.9, c = 38.1$ Å, tetragonal). Figs. 5(a), (b) and (c), (d) are the diffraction profiles of the three-beam cases $(000, 0\bar{1}3, \bar{2}\bar{3}\bar{1})$ and $(000, 01\bar{3}, 231)$ and the four-beam cases $(000, 003, 0\bar{1}1, 0\bar{1}2)$ and $(000, 00\bar{3}, 01\bar{1}, 01\bar{2})$ of the organic crystals, respectively. Figs. 5(a) and (b) are obtained with synchrotron radiation and Figs. 5(c) and (d) with a rotating-anode X-ray source. In Figs. 5(a) and (b), the peak position x_o, labeled as $\Delta\psi = 0$, is determined by minimizing the difference between $I'_G(x_o)$ and $I'_G(x_o + \eta/2) + I'_G(x_o - \eta/2)$, where $\eta = 0.02^\circ$ for both the profiles in Figs. 5(a) and (b). $C = [I'_G(a) + I'_G(b)]/2 = -0.02$ at $\Delta\psi = 0$, where a and b refer to the values of I'_G in Figs. 5(a) and (b). With these values of C, x_o and η, the phase-independent $I_K(\Delta\psi)$ can be constructed. By subtracting $I_K(\Delta\psi)$ from $I'_{Ga}(\Delta\psi)$ and $I'_{Gb}(\Delta\psi)$, the phase-dependent $I_{Da}(\Delta\psi)$ and $I_{Db}(\Delta\psi)$ can thus be obtained. From the intensities I_D at $\pm\eta/2$, *i.e.* $I_+(a) = 0.007$, $I_-(a) = -0.042$, $I_+(b) = 0.011$ and $I_-(b) = -0.003$, the phase values determined according to (11) are $\delta_{3,a} = 36^\circ$ and $\delta_{3,b} = -30^\circ$, compared with the theoretical values of 35 and -35°. It should be noted that the entire profile of each intensity

distribution involved has been used for the phase analysis.

The phase-determination procedures can also be applied to four-beam diffraction involving a 2 or 2_1 rotation axis. Because the relative diffracted intensity of a four-beam case depends on two effective structure-factor triplets, the phases of the two triplets are identical only when a 2 or 2_1 rotation axis is present (Hümmer *et al.*, 1991). Under this condition, the phases can be quantitatively analyzed. For example, in Figs. 5(*c*) and (*d*), the two four-beam cases of the organic crystal involve a twofold rotation axis, [003] or [00$\bar{3}$], so that the triplet phases can be determined in the same way as in three-beam cases. The determined phases are $\delta_{3,c} = 176°$ and $\delta_{3,d} = 167°$, compared with the theoretical values of 180°. Figs. 6(*a*)–(*d*) are the scans of the two centrosymmetrically related four-beam cases (000, 550, 120, 340/000, $\bar{5}\bar{5}0$, $\bar{1}\bar{2}0$, $\bar{3}\bar{4}0$) and (000, 550, 542, 102/000, $\bar{5}\bar{5}0$, $\bar{5}\bar{4}\bar{2}$, $\bar{1}0\bar{2}$) of lysozyme, obtained using a rotating-anode X-ray source. Since 550 and $\bar{5}\bar{5}0$ are the primary reflections, the crystal rotations are along twofold axes. By the same token, the corresponding triplet phases $\delta_3(E)$ can be determined experimentally as

$$\delta(\bar{5}\bar{5}0) + \delta(120) + \delta(430) = 12°,$$
$$\delta(550) + \delta(\bar{1}\bar{2}0) + \delta(\bar{4}\bar{3}0) = -7°,$$
$$\delta(\bar{5}\bar{5}0) + \delta(542) + \delta(01\bar{2}) = -74°,$$
$$\delta(550) + \delta(\bar{5}\bar{4}\bar{2}) + \delta(0\bar{1}2) = 88°,$$

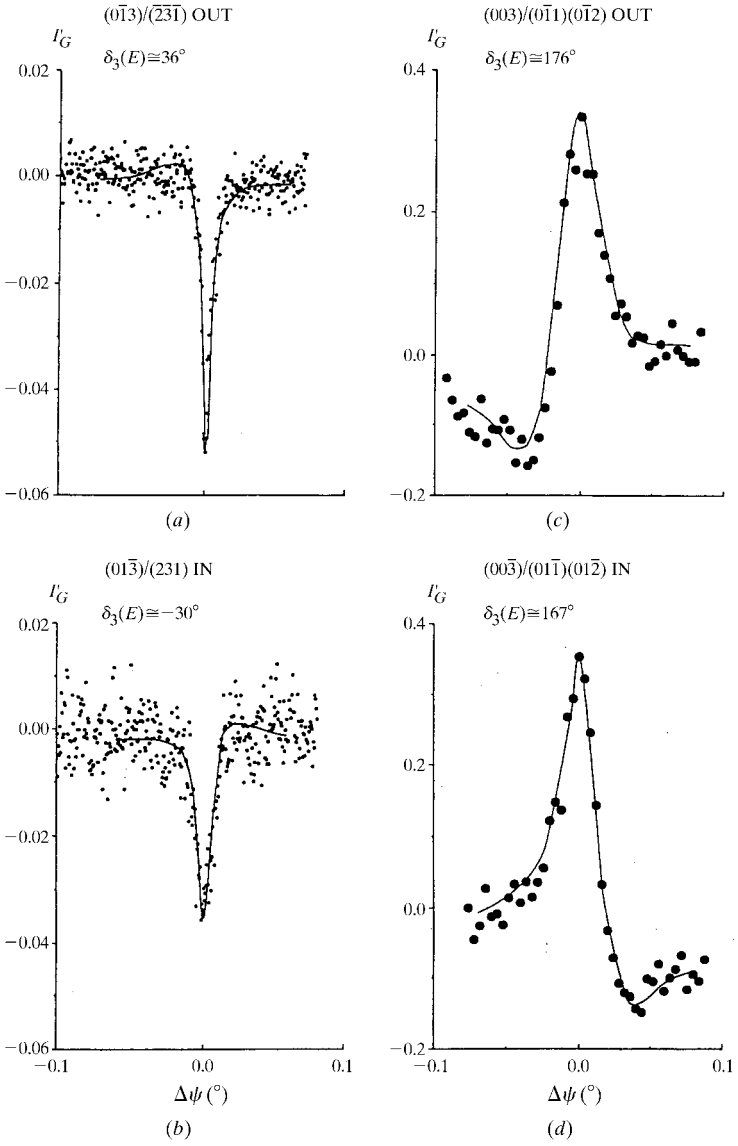

Fig. 5. Three-beam diffraction profiles: (*a*) (000, 0$\bar{1}$3, $\bar{2}$3$\bar{1}$) and (*b*) (000, 01$\bar{3}$, 231) with synchrotron radiation ($\lambda = 1.54134$ Å); four-beam profiles: (*c*) (000, 003, 0$\bar{1}$1, 0$\bar{1}$2) and (*d*) (000, 00$\bar{3}$, 01$\bar{1}$, 01$\bar{2}$) with Cu $K\alpha_1$ radiation ($\lambda = 1.54056$ Å) of $C_{25}H_{25}NO$.

compared, respectively, with the theoretical values of 0, 0, −72 and 72°, calculated from the known structure of lysozyme (Diamond *et al.*, 1974). The overall errors in δ_3 for the cases analyzed are about 30° (Huang *et al.*, 1994).

5. Discussions and conclusions

The accuracy of the quantitative *N*-beam phase-determination procedure depends on the measured peak width, the peak intensity and, more importantly, the peak position of $\Delta\psi = 0$. With the intensity minimization procedure mentioned for determining the peak position of $\Delta\psi = 0$, the accuracy of the determined phase values achieved can be within 30°. For higher-order *N*-beam cases ($N > 4$), if many weak reflections are involved, these higher-order diffractions can be treated as three-beam or four-beam cases. Case studies for phase determination in centrosymmetric crystals using multiple diffraction up to the eight-beam case ($N = 8$) have been demonstrated (Post *et al.*, 1986; Chang *et al.*, 1988).

The *N*-beam phasing method is based on the effects of dynamical interaction in perfect or nearly perfect crystals. Doubts have been raised as to whether such a method is useful for phase determination in organic or macromolecular crystals that are usually not perfect. As depicted in Figs. 5 and 6 and described in the report by Hümmer *et al.* (1991), the *N*-beam diffractions from these crystals still show *N*-beam phase effects on the intensity distributions. This is because within the crystal sample there are many tiny perfect crystal blocks that can diffract dynamically, thus the coherent interaction of the X-ray wave field is maintained. Therefore, the *N*-beam phasing method has been successfully employed to determine the absolute configuration of crystals (Marthinsen & Hoier, 1986; Hümmer & Weckert, 1995) and has even been applied to phase determination for quasicrystals (Lee *et al.*, 1993; Weckert & Hümmer, 1997, and references therein).

Although the *N*-beam phasing method is capable of determining X-ray reflection phases qualitatively and quantitatively, there are still difficulties to be overcome before it can become a practical method for routine crystal-structure analysis. The main obstacle is that to collect *N*-beam diffraction profiles using the Renninger technique is very time consuming, especially for macromolecular crystals. To eliminate such an obstacle, a fast collection of *N*-beam diffraction profiles using two-dimensional imaging techniques, like Kossel, accompanied by a synchrotron X-ray source may be required. Yet appropriate imaging techniques need to be developed. The conventional crystal-rotation and oscillation techniques at multibeam condition may be candidates.

Phase extension *via* other available mathematical methods, such as direct methods, maximum entropy and the simulated-annealing method (Su, 1995), is another possibility for quickly developing more known phases until reaching a critical number for structure determination at a desired resolution.

The *N*-beam phasing method is not limited to three-dimensional structures of single crystals. In principle,

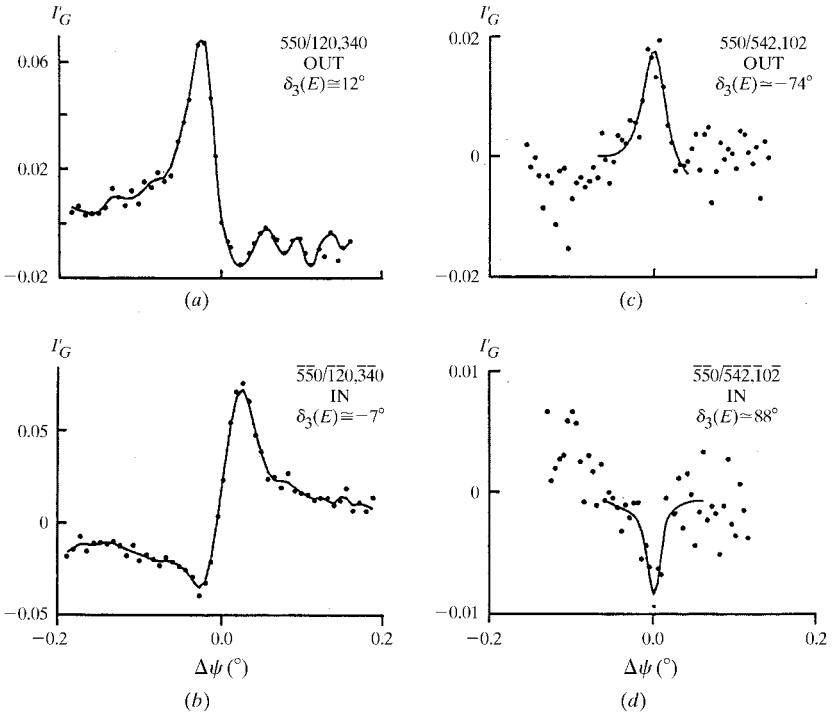

Fig. 6. Four-beam profiles of a tetragonal lysozyme using Cu $K\alpha_1$ radiation ($\lambda = 1.54056$ Å).

N-beam diffraction can take place in two-dimensional or quasi-two-dimensional structures like surfaces and interfaces. Recently, a three-beam diffraction at grazing incidence has been realised for crystal surface in-plane reflections using photon-energy scans with synchrotron sources. The phase determination of in-plane reflections has been demonstrated (Chang *et al.*, 1998). This adds another potential application of this phasing method to structure-related studies.

The author is indebted to the National Science Council, Taiwan, the Republic of China, for support during the course of the related research.

References

Authier, A., Lagomarsino, S. & Tanner, B. K. (1996). Editors. *X-ray and Neutron Dynamical Diffraction – Theory and Applications.* New York: Plenum Press.
Batterman, B. W. & Cole, H. (1964). *Rev. Mod. Phys.* **36**, 681–717.
Bricogne, G. & Gilmore, C. J. (1990). *Acta Cryst.* A**46**, 284–297.
Caticha-Ellis, S. (1969). *Acta Cryst.* A**25**, 666–673.
Chang, S. L. (1982). *Phys. Rev. Lett.* **48**, 163–166.
Chang, S. L. (1984). *Multiple Diffraction of X-rays in Crystals.* Berlin: Springer-Verlag.
Chang, S. L. (1987). *Crystallogr. Rev.* **1**, 87–189.
Chang, S.-L., Huang, Y. S., Chao, C. H., Tang, M. T. & Stetsko, Y. (1998). *Phys. Rev. Lett.* **80**, 301–304.
Chang, S. L., Hung, H. H., Luh, S. W., Pan, H. H., Tang, M. T. & Sasaki, J. M. (1988). *Acta Cryst.* A**44**, 63–70.
Chang, S. L., King, H. E., Huang, M. T. & Gao, Y. (1991). *Phys. Rev. Lett.* **67**, 3113–3116.
Chang, S. L. & Tang, M. T. (1988). *Acta Cryst.* A**44**, 1065–1072.
Chapman, L. D., Yoder, D. R. & Colella, R. (1981). *Phys. Rev. Lett.* **46**, 1578–1580.
Cole, H., Chambers, F. W. & Dunn, H. M. (1962). *Acta Cryst.* **15**, 138–144.
Colella, R. (1974). *Acta Cryst.* A**30**, 413–423.
Colella, R. (1992). *P. P. Ewald and his Dynamical Theory of X-ray Diffraction*, edited by D. W. J. Cruickshank, H. J. Juretschke & N. Kato, pp. 71–78. Oxford: IUCr/Oxford University Press.
Diamond, R., Phillips, D. C., Blake, C. C. F. & North, A. J. C. (1974). *J. Mol. Biol.* **82**, 371–391.
Ewald, P. P. (1965). *Rev. Mod. Phys.* **37**, 46–56.
Ewald, P. P. & Heno, Y. (1968). *Acta Cryst.* A**24**, 5–15.
Hargittai, I. (1998). *Acta Cryst.* A**54**, 697–706.
Hendrickson, W. A. (1991). *Science*, **254**, 51–58.
Hoier, R. & Marthinsen, K. (1983). *Acta Cryst.* A**39**, 854–860.
Huang, M. T., Wang, C. M. & Chang, S. L. (1994). *Acta Cryst.* A**50**, 342–344.
Hümmer, K. & Billy, H. W. (1982). *Acta Cryst.* A**38**, 841–848.
Hümmer, K. & Billy, H. W. (1986). *Acta Cryst.* A**42**, 127–133.
Hümmer, K., Bondza, H. & Weckert, E. (1991). *Z. Kristallogr.* **195**, 169–188.
Hümmer, K., Schwegle, W. & Weckert, E. (1991). *Acta Cryst.* A**47**, 60–62.
Hümmer, K. & Weckert, E. (1990). *Acta Cryst.* A**46**, 534–536.
Hümmer, K. & Weckert, E. (1995). *Acta Cryst.* A**51**, 431–438.
Juretschke, H. J. (1982*a*). *Phys. Rev. Lett.* **48**, 1487–1489.
Juretschke, H. J. (1982*b*). *Phys. Lett.* A**92**, 183–185.
Juretschke, H. J. (1986). *Phys. Status Solidi B*, **135**, 455–466.
Kato, N. (1974). *X-ray Diffraction*, edited by L. V. Azaroff, pp. 176–438. New York: McGraw-Hil.
Kossel, W. (1936). *Ann. Phys. (Leipzig)*, **26**, 533–553.
Lee, H., Colella, R. & Chapman, L. D. (1993). *Acta Cryst.* A**49**, 600–605.
Lipscomb, W. N. (1949). *Acta Cryst.* **2**, 193–194.
Marthinsen, K. & Hoier, R. (1986). *Acta Cryst.* A**42**, 484–492.
Mo, F., Hauback, B. C. & Thorkildsen, G. (1988). *Acta Chem. Scand. Ser. A*, **42**, 130–138.
Moon, R. M. & Shull, C. G. (1964). *Acta Cryst.* **17**, 805–812.
Pinsker, Z. G. (1978). *Dynamical Scattering of X-rays in Crystals.* Berlin: Springer-Verlag.
Post B. (1977). *Phys. Rev. Lett.* **39**, 760–763.
Post, B., Gong, P. P., Kern, L. & Ladell, J. (1986). *Acta Cryst.* A**42**, 178–184.
Renninger, M. (1937). *Z. Kristallogr.* **97**, 107–121.
Rossmann, R. G. (1972). Editor. *The Molecular Method.* New York: Gordon and Breach.
Schenk, H. (1991). Editor. *Direct Methods for Solving Crystal Structures.* New York: Plenum Press.
Shen, Q. (1986). *Acta Cryst.* A**42**, 525–533.
Shen, Q. & Finkelstein, K. D. (1990). *Phys. Rev. Lett.* **65**, 3337–3340.
Su, W. P. (1995). *Acta Cryst.* A**51**, 845–849.
Tang, M. T. & Chang, S. L. (1988) *Acta Cryst.* A**44**, 1073–1078.
Tang, M. T. & Chang, S. L. (1990). *Phys. Lett.* A**143**, 405–408.
Thorkildsen, G. (1987). *Acta Cryst.* A**43**, 461–369.
Weckert, E. & Hümmer, K. (1990). *Acta Cryst.* A**46**, 387–393.
Weckert, E. & Hümmer, K. (1997). *Acta Cryst.* A**53**, 108–143.
Woolfson, M. M. & Fan, H.-F. (1995). *Physical and Non-physical Methods of Solving Crystal Structures.* Cambridge University Press.
Zachariasen, W. H. (1965). *Acta Cryst.* **18**, 705–710.